

1 **Chaotic breccia zones on the Pembroke Peninsula, South Wales: evidence for collapse**
2 **into voids along dilational faults**

3

4 **N.H. Woodcock^{*}, A.V.M. Miller, C.D. Woodhouse**

5

6 Department of Earth Sciences, University of Cambridge, Cambridge CB2 3EQ, UK

7

8 * Corresponding author: nhw1@cam.ac.uk, +441223 333430

9

10

11 **Abstract**

12

13 Chaotic breccias and megabreccias – locally called gash breccias – hosted within the
14 Pembroke Limestone Group (Visean, Mississippian, lower Carboniferous) of southwest
15 Wales are re-mapped along with spatially-related crackle and mosaic breccias. Of thirteen
16 studied megabreccia bodies, seven lie along steep, NNW- or NNE-striking strike-slip faults
17 originating during north-south Variscan (late Carboniferous) shortening, though reactivated
18 during later extension. Four bodies are conformable with E-W striking, steeply-dipping
19 bedding, and two have irregular or indeterminate margins. The bedding-parallel zones are
20 interpreted as the dilational tips of listric normal faults, and the cross-strike faults as
21 transtensional transfer zones. Sub-horizontal clast fabrics suggest brecciation by gravitational
22 collapse into opening fissures rather than by cataclasis along the faults. Most fissures have
23 geometrically matched margins produced by this dilational faulting, and only locally have the
24 indented margins indicating solutional processes. The most likely age for the main fissure
25 extension and fill is late Triassic, based on analogous dated fills at the eastern end of the

26 Bristol Channel Basin. The Pembroke megabreccias blur the distinction between fault rocks
27 formed by deformation and those formed by redeposition along fault zones.

28

29 *Keywords:* megabreccia, fault rocks, dilational fault, Bristol Channel Basin.

30

31

32

33 **1. Introduction**

34

35 Breccias, rocks made of coarse angular fragments, form by a range of sedimentary, magmatic
36 and deformational processes (e.g. Laznicka, 1988). They commonly have a high porosity and
37 permeability, and are therefore economically important as hosts and conduits for
38 groundwater, hydrocarbons or mineralization. The origin of some breccias can be deduced
39 from their texture, composition and context but the origin, or even the three-dimensional
40 geometry, of other breccias is uncertain.

41 One problematic breccia formation mechanism is gravitational collapse into voids formed
42 by solution (Loucks, 1999) or by mismatch of fault walls (e.g. Woodcock et al., 2006; Ferrill
43 et al., 2011; Walker et al., 2011). This collapse mechanism grades into other processes:
44 confined implosion at pressure-release zones along faults (e.g. Sibson, 1986) and phreato-
45 magmatic explosion in igneous and hydrothermal settings. One area where all these
46 mechanisms have been proposed for the same suite of breccias is the Pembroke Peninsula,
47 south Wales (review by Walsh et al., 2008) where chaotic megabreccias (e.g. Fig. 4d, e),
48 locally called gash breccias, are hosted within lower Carboniferous (Mississippian)
49 limestones. This paper reports new work on the megabreccias and on spatially related fault
50 breccias that clarifies the origin of many of the occurrences.

51

52

53 **2. Geological setting of the studied breccias**

54

55 The Pembroke Peninsula, west Wales, lies close to the northern limit of strong Variscan
56 (late Carboniferous) deformation in Britain (Fig. 1b; British Geological Survey, 1996). The
57 mid-Ordovician to late Carboniferous sequence is deformed into E-W trending upright folds
58 with kilometric wavelengths (Fig. 1a). The studied breccias occur in the Pembroke Limestone
59 Group (Tournaisian and Viséan), which crops out in three major synclines: the St Florence,
60 Pembroke and Bullslaughter Bay Synclines. The folds are cut by two conjugate sets of strike-
61 slip faults striking NNW and NNE (Fig. 1a). The peninsula is geologically bounded to the
62 north by the steeply S-dipping Ritec Fault, with a reverse throw of 0.5 to 1 kilometre.

63

64 [Figure 1 about here]

65

66 Thirty localities have been studied, all but two of them coastal. Most are accessible either
67 at shore level or at the top of the 50 metre high cliffs, although some can only be reached or
68 viewed from the sea.

69 The stratigraphic distribution of breccias within the Pembroke Group reflects its
70 lithological contrasts (Fig. 2). No megabreccias occur in the lower units, which are
71 dominantly shale-prone thin- or medium-bedded limestone. Megabreccias are common where
72 mechanically strong thick-bedded limestone dominates: particularly in the High Tor and
73 Cornelly formations (Arundian to Holkerian) of the northern areas and the Stackpole and
74 Oxwich Head formations (Holkerian to Asbian) of the southern area. However, overlying

75 thinner-bedded units are also brecciated: the Stormy Limestone Formation (Holkerian) in the
76 north and the Oystermouth Formation (Brigantian) in the south.

77

78 [Figure 2 about here]

79

80 **3. Previous work and hypotheses**

81

82 The history of research on the Pembrokeshire megabreccias has been reviewed by Walsh et
83 al. (2008). Early research produced two genetic hypotheses. Dixon (1921) envisaged karstic
84 solution of limestone, producing large voids into which wall and roof rocks progressively
85 collapsed (Fig. 3a). By contrast, Hancock (1964) and Thomas (1970, 1971) proposed
86 formation by tectonic fragmentation along faults (Fig. 3b). Walsh et al. (2008) concluded that
87 the megabreccias were formed by more than one mechanism, and suggested a third: phreatic
88 explosion due to upward escape of thermally-driven superheated fluids (Fig. 3d). Rowberry et
89 al. (2014) and Błazejowski and Walsh (2013) showed that, at Bullslaughter Bay (localities 3
90 and 4), chemically aggressive fluids, either deep or meteoric, have produced substantial
91 residual deposits, which apparently overprint chaotic breccias and bedded sequences.

92

93 [Figure 3 about here]

94

95 Recent studies on chaotic breccia hosted within Carboniferous limestone elsewhere in the
96 UK provide analogues for the Pembrokeshire examples. Woodcock et al. (2006) attributed
97 megabreccia along the Dent Fault, northwest England, to collapse of voids produced by
98 dilational fault displacement (Fig. 3c). Wright et al. (2009) studied strike-slip cross faults in
99 the Pembroke Group of the Gower Peninsula, there contain void-filling veins and breccias

100 produced during active faulting rather than by solution. One of the westernmost faults
101 contains megabreccia identical to the Pembrokeshire examples. Eastward from Gower,
102 sediment-filled extensional fissures cut the Pembroke Group in the Mendip Hills (Wall and
103 Jenkyns, 2004). Rather than megabreccia, these fills are dominated by Triassic and Early
104 Jurassic sediment infiltrated from the contemporary land surface.

105

106

107 **4. Breccia zone lithologies**

108

109 *4.1 Terminology*

110

111 The studied zones contain a range of breccias, particularly some with very large clasts (over
112 1 metre in diameter) referred to informally as *megabreccias*. Sedimentologically, such large-
113 clast breccias would be termed *boulder breccia*. The genetic term *gash breccia* is avoided, as
114 pre-supposing that the breccias formed in an open void.

115 The breccias are classified using the non-genetic scheme developed for cave-collapse
116 zones (e.g. Loucks, 1999) as modified for fault zones (Mort and Woodcock, 2008; Woodcock
117 and Mort, 2008). The spectrum from *crackle breccia* through *mosaic breccia* to *chaotic*
118 *breccia* simply reflects increasing disaggregation of the protolith, and therefore decreasing
119 percentage of large (>2 mm) clasts in the overall rock volume. Breccias can either contain a
120 fine-grained matrix or carbonate cement. This classification is suitable for any breccia and its
121 use here does not pre-judge whether or not the Pembrokeshire breccias were formed along
122 faults.

123

124 *4.2 Crackle and mosaic breccia*

125

126 Crackle and mosaic breccia has angular clasts with a fitted-fabric texture and only limited
127 separation and rotation of clasts. In crackle breccia (Fig. 4a) the porosity between large
128 (>2 mm) clasts is less than 25% of the rock volume, whereas in mosaic breccia (Fig. 4b) it is
129 about 25-40%. The porosity is filled either by crystalline carbonate cement or by fine
130 (<2 mm) matrix, both detailed below (section 4.5, 4.6). Crackle and mosaic breccia typically
131 occur at the gradational margins to chaotic breccia zones, with calcite cement between the
132 clasts. Pods of crackle and mosaic breccia may be interleaved on a scale too fine to
133 distinguish separately on the maps of individual fault zones (sections 6 to 9).

134

135 [Figure 4 about here]

136

137

138 *4.3 Chaotic breccia and megabreccia*

139

140 Chaotic breccia and megabreccia (Fig. 4c) has angular to sub angular clasts that lack a fitted-
141 fabric texture. Clasts have been rotated and translated enough to obscure any match with each
142 other. Nevertheless, all the chaotic breccias zones are monomict; that is their large clasts are
143 entirely derived from the Pembroke Group. Indeed, in all but one zone, the clasts derive from
144 the same limestone formation that hosts the breccia. The exception is at Trevalen (locality 7)
145 where a breccia hosted in thickly-bedded Stackpole and Oxwich Head limestones also
146 contains clasts from the overlying thinner-bedded Oystermouth Formation. Very large (1 to
147 10 metre) clasts in megabreccia may be equidimensional, or more typically bedded slabs with
148 their long dimension parallel to their bedding (Figs 4d, e). As in mosaic breccia, the porosity

149 in chaotic breccia can be filled either by carbonate cement or by fine-grained matrix, both
150 detailed below (section 4.5, 4.6), or remain unfilled.

151

152 *4.4 Cataclasite*

153

154 The cores of some faults have thin (<1 metre) zones of cataclasite or fine matrix-rich chaotic
155 breccia (Fig. 4f). On the fault-rock scheme of Woodcock and Mort (2008), the boundary
156 between these two rocks types is at 2 mm average clast size, although other authors have used
157 a smaller clast size, for instance Higgins (1971) at 0.2 mm and the North American Geologic-
158 map Data Model (2004) at 0.1 mm. These fault rocks lack a foliation, although they may be
159 cut by anastomosing principal slip surfaces within the fault core.

160

161 *4.5 Carbonate cement*

162

163 The dominant cement is calcite, occurring in two growth forms. *Blocky calcite* (Fig. 5a)
164 comprises equidimensional crystals about 1 cm in diameter. *Elongate blocky calcite* (Fig. 5a,
165 b) forms acicular crystals up to 5 cm long. Both forms have euhedral crystal terminations,
166 showing that they grew into fluid-filled voids. Both calcite types nucleate on clasts and void
167 walls, with the elongate calcite forming conspicuous radiating crystal masses. In places,
168 clasts in 2D view are completely surrounded by radiating cement, forming *spar balls* (Fig
169 5b), although the possibility that such clasts are supported by other clasts in the third
170 dimension cannot be ruled out. If not, the formation of these structures is problematic (Genna
171 et al., 1996; Frenzel and Woodcock, in press).

172 Growth of equant, rather than elongate, crystals reflects high nucleation rates from

173 hydrothermal fluids, probably due to fluid supersaturation (Oliver and Bons, 2001), arising

174 from arrest of a rising mass of fluid (Bons, 2001) or by a rapid drop in fluid pressure during
175 hydraulic fracture (Phillips, 1972). Because cements are void-filling rather than keeping pace
176 with void opening, opening rates must have exceeded precipitation rates.

177 Although most carbonate cement is non-ferroan, small volumes of ferroan calcite fill late-
178 stage porosity or form thin cross-cutting veins. Ferroan dolomite nodules occur (Walsh et al.,
179 2008) in the breccia zones at Draught (locality 13, Fig. 2). The nodules are brecciated and
180 recemented by calcite.

181

182 [Figure 5 about here]

183

184 *4.6 Sediment matrix and laminated infill*

185

186 Where breccia clasts have a matrix (<2 mm) infill, this typically comprises calcitic particles
187 between silt and medium sand grade (Fig. 5c). Most sediment is coloured red by hematite or
188 brown by limonite. Lamination is typically visible wherever voids are wider than a few
189 centimetres. It has a concave-up catenary form (Fig. 5c) consistent with lamina-by-lamina
190 deposition within each void. Where sediment and cement occur together within a void, the
191 sediment is the earlier fill. The sediment occupies the lower part of voids or has accumulated
192 above tabular clasts (Fig. 5d), and the contact of the sediment and overlying cement forms a
193 geopetal indicator. All geopetal and way-up evidence suggests that the host breccia zones
194 have not been significantly rotated since they were formed.

195 Several laminated sediment fills are of particular significance.

196 *Laminated and thinly-bedded crinoidal grainstone* occurs at Draught (locality 13). The
197 crinoids cannot be dated. Their articulated and non-corroded shapes might question
198 reworking from local well-cemented Carboniferous rocks although Rowberry et al. (2014)

199 record crinoid ossicles and Brigantian conodonts (Błażejowski and Walsh, 2013) in karstic
200 weathering residues at Bullslaughter south (locality 4). Alternatively, Mesozoic crinoids are a
201 conspicuous component of the Mendips fissure fills (Wall and Jenkyns, 2004), where they
202 infiltrated in sediment from the Mesozoic sea floor.

203 *Well-cemented laminated micrite* forms prominent catenary-bedded sheets at some
204 localities (e.g. Draught), where it is more resistant to weathering than wall rocks (Fig. 5e). In
205 thin section it is seen to comprise calcite debris cemented by ferroan calcite and dolomite.
206 This is the lithology confusingly termed ‘stalagmite’ by Dixon (1921) and also by Thomas
207 (1971) and Walsh et al. (2008). However, the latter authors consider that the deposits are not
208 phreatic zone speleothem but rather a form of hot-water travertine. By contrast, we do not
209 attach any special significance to these sediments: they are merely well-cemented examples
210 of normal sediment infill.

211

212

213 *4.7 Residual deposits from weathering overprint*

214

215 At Bullslaughter Bay, a deep weathering episode has converted both bedrock and breccias
216 into residual deposits (Błażejowski and Walsh, 2013; Rowberry et al., 2014). Mudstones
217 assigned to the late Visean Aberkenfig Formation (Błażejowski and Walsh, 2013) or the
218 Namurian Bishopton Mudstone Formation (Walsh et al., 2008) have been kaolinised and
219 were termed *saprolite* by Walsh et al. (2008). Chert interbeds have been brecciated but define
220 relict bedding. Whether the brecciation results from *in situ* weathering (Rowberry et al.,
221 2014) or involves phreatic explosive disruption (Błażejowski and Walsh, 2013) is debated. It
222 is similarly unclear to what extent brecciation in the underlying Oystermouth Formation
223 predated or accompanied deep weathering. For instance, one interpretation of a breccia at

224 Bullslaughter south (locality 4, Fig. 5f) is as a laminated sand deposited in a void, and
225 punctured by limestone ‘dropstones’ from the hanging wall. An alternative explanation
226 (Błazejowski and Walsh, 2013; Rowberry et al., 2014) is that the lamination is inherited from
227 decalcified limestone, with the blocks as less weathered relicts. Such textures are termed
228 *ghost karst* (Dubois et al., 2014). The context of the residual deposits at Bullslaughter Bay is
229 discussed later (Sections 6.2, 9).

230

231

232 **5. Distribution and context of breccia bodies**

233

234 Figure 6 shows which lithologies are important at each locality, grouped according to its
235 structural setting. Most lithologies occur in every setting, but chaotic megabreccias do not
236 occur along thrusts, and cataclasites do not occur in irregular breccia bodies. The tabulated
237 widths of zones vary from 5 to 200 metres, and do not correlate closely with structural
238 setting.

239

240 [Figure 6 about here]

241

242 Three end-member structural settings can be recognised (Fig. 7):

243 a) zones that strike parallel to bedding (roughly east-west), either parallel also to bedding dip
244 or to cross-cutting thrust faults;

245 b) zones along steep NNW or NNE-striking faults that cut across bedding strike; and

246 c) zones with irregular margins that parallel neither faults nor bedding.

247 A triangular diagram (Fig. 7) shows semiquantitatively the range of geometry between
248 the three end members. Three breccia zones have geometries too uncertain to plot but, of the

249 27 plotted examples, over half (15) are closely related to cross-strike faults, 5 parallel
250 bedding and 3 parallel thrust-faults. The remaining 4 have mostly irregular margins. These
251 groupings provide a framework for detailing the structural geometry of representative breccia
252 zones (sections 6 to 9).

253

254 [Figure 7 about here]

255

256

257 **6. Breccias associated with cross-strike faults**

258

259 *6.1. Cross-fault zones with simple geometry*

260

261 Nine vertical cross-strike fault zones have simple geometries and cluster at the top corner of
262 Figure 7. Maps of three examples (Fig. 8a-d and 9a) show that one or both margins grade
263 inwards from crackle through mosaic breccia into a fault core of chaotic breccia or
264 megabreccia. Typically one principal slip surface cut through or bounds this central fault
265 core. Fine-grained cataclasite occurs in the core in one only case (Stackpole, Fig. 8c, d).

266

267 [Figure 8 about here]

268

269 Six steeply-dipping cross-strike fault zones have complex geometries, with greater
270 outcrop widths and more than one mappable fault core. The example at Flimston Bay (loc. 1,
271 Fig. 8e, f) occurs along a NNW-striking fault with at least 500 m of dextral strike-slip offset
272 of the Bullslaughter Bay Syncline. The example at Bullslaughter east (loc. 3, Fig. 10a, c) has
273 three principal slip surfaces marked by chaotic breccia and megabreccia, separated by screens

274 of intact limestone. Draught Cove (loc. 14, not illustrated) contains at least nine principal slip
275 surfaces, seven chaotic breccias zones, three cataclasite zones and two zones of chaotic
276 megabreccia.

277 In general then, the cross-strike faults host the thickest and most complex breccia zones
278 (Fig. 6). They coincide with cross-faults mapped in the detailed survey by Dixon (1921).
279 Independent evidence of strike-slip displacement is available where the faults laterally
280 displace fold axial planes, for instance at localities 1, 2, 3, 4 and 12, and on about ten other
281 faults detailed by Dixon (1921, 181-185). The sense of displacement is dextral on the NNW
282 faults and sinistral on the NNE faults. This pattern is so well defined that it was the main
283 example cited by Anderson (1951) for his classic stress interpretation of conjugate sets of
284 strike-slip faults. The faults formed in response to north-south directed maximum principal
285 stress during the Variscan event. These faults would have been transpressional during
286 Variscan shortening, and not natural hosts for chaotic breccias that require dilation of the
287 fault zone. An extensional phase during latest Variscan or later time is implied by regional
288 evidence (Section 12.5).

289 Sub-horizontal slickensides and slickencrysts are additional evidence that the breccia
290 zones coincide with strike-slip faults. Examples have been observed at localities 1, 5 and 14,
291 and Dixon (1921, p. 182) states that “all the slickensiding that has been examined along the
292 faults shows either horizontality or only a gentle inclination in the striae or fluting produced
293 by the movement.” It might still be argued that some of the chaotic breccias are a later infill
294 to karstic solution cavities along the faults. However, examples such as the low displacement
295 splay fault at Stackpole Quay (loc. 12, Fig. 8c, d) argue against solution as a general genetic
296 model. The fault walls and enclosed fragments fit back together perfectly, in contrast to the
297 irregular, sculpted and mismatching fissure walls that would be produced by solution of the
298 limestone.

299

300

301 **7. Breccias associated with thrust faults**

302

303 Breccia zones that parallel bedding strike (Fig. 7, bottom left) fall into two types. Three
304 zones, described in this section, are clearly associated with faults, in that they cut across the
305 dip of bedding, show stratigraphic displacement, host cataclasite zones, or contain
306 slickensided surfaces. A further five zones, (section 8) lack these four criteria and are
307 conformable with bedding dip as well as strike.

308 The best example of a strike-parallel thrust zone is at Tenby east (loc. 25, Fig. 9a), where
309 the 19 km long Ritec Fault meets the coast. It dips steeply southward, with a reverse throw of
310 about 450 m in the east of Pembrokeshire and 900 m in the west (Dixon, 1921). At Tenby a
311 zone of crackle and mosaic breccia contains two 10-30 m wide thrust zones of cataclasite.
312 Other possible thrust faults have lower displacements. At Barafundle Bay (loc. 11), a small
313 south-dipping fault with chaotic and crackle breccia may be a minor limb thrust near a fold
314 hinge (Dixon, 1921, p. 180).

315 The relative rarity of chaotic breccia and absence of megabreccia, along thrust faults is
316 notable. It suggests that a dilational component to faults is necessary for megabreccia
317 formation.

318

319

[Figure 9 about here]

320

321 **8. Bedding sub-parallel breccias**

322

323 By contrast with its absence in thrust zones, megabreccia is hosted in four out of five zones
324 with contacts that parallel bedding dip as well as strike (Fig. 7). A typical zone at Nanna's
325 Cave (loc. 29, Fig. 9b, c) has a central zone of chaotic megabreccia bordered by several
326 metres of chaotic breccia. The flanking limestone beds, which dip about 80°, are scarcely
327 brecciated, with just a 3m wide zone of crackle breccia within the northern wall, hosts an
328 open angular kink fold of bedding (Fig. 9c).

329 Lydstep Point (loc. 16, Fig. 9d, g) and Whitesheet (loc. 15, Fig. 9d, e, f) are wider zones
330 with the same basic geometry, including non-brecciated, but kinked wall rock south of the
331 Whitesheet mass (Fig. 9e). The two breccia bodies do not appear to join up along strike, but
332 are terminated by cross faults. The Whitesheet breccia is itself cut by later cross-strike faults,
333 one hosting cataclasite. Although most margins of the five breccias zones in this category
334 precisely parallel bedding, those at Trevalen (loc. 7, not illustrated) weakly transgress the
335 bedding, particularly in the hangingwall. This is probably related to the lower bedding dips
336 (40° to 70°) in this example.

337 The sharp planar contacts and the lack of brecciation in the adjacent limestones to the
338 bedding-parallel breccia zones suggest that they formed by extension perpendicular to
339 bedding rather than by shear parallel to it or solution within it. The angular kink folds at the
340 margins of several zones indicate one way in which bedded limestone beds collapsed during
341 extension. The amount of extension was small enough that it could dissipate in a short
342 distance along strike or at a synchronous cross fault.

343

344 **9. Irregular breccia masses**

345

346 Four breccia zones have irregular margins, not obviously concordant with either bedding
347 or faults (Fig. 7, bottom right). Incomplete exposure leaves open the possibility that some of
348 their margins are more regular.

349 The largest such zone, at Bullslaughter west (loc. 2, Fig. 10a, b), maps out as an
350 equidimensional pod of chaotic megabreccia, grading laterally into chaotic breccia. The
351 southern and eastern margins are faulted, but with different fault strikes. Three separate
352 breccia bodies are designated as Bullslaughter south (loc. 4, Fig. 10a). The northernmost
353 body is an E-W matrix-rich megabreccia zone with a faulted northern margin. The central
354 body comprises the crackle-brecciated, kaolinised cherty mudstones, termed saprolite by
355 Walsh et al. (2008). The consensus is now that these are deeply weathered late Viséan
356 mudstones in the hinge zone of the Bullslaughter Bay Syncline (Dixon, 1921; Thomas, 1971;
357 Walsh et al., 2008; Błazejowski and Walsh, 2013; Rowberry et al., 2014), with bedding
358 obliterated by kaolinisation and brecciation. The southern breccia zone is of chaotic breccia
359 and hematitic sand (Fig. 5f). The body has irregular contacts with the host limestones,
360 transecting an anticline-syncline pair. This is the deposit already discussed (Section 4.7) in
361 which the structures could either be interpreted as due to sedimentation and collapse into a
362 void or as *in situ* weathering to give ghost karst .

363

364 [Figure 10 about here]

365

366 It is difficult to generalise from the breccia bodies with irregular margins, and it is
367 possible that each of the examples at Bullslaughter Bay has contrasting origins. Irregular
368 margins are characteristic of solutional processes, whether to form voids for subsequent

369 breccia infill, to generate in situ brecciation by heterogeneous weathering, or to overprint
370 earlier structures and textures. The good examples of solutional processes at Bullslaughter
371 Bay contrast with the general paucity of such processes in other breccia zones in
372 Pembrokeshire.

373

374

375 **10. Geometric clues to megabreccia formation**

376

377 Dixon (1921 p.158) and Walsh et al. (2008 p.139) regarded the clast fabric in the chaotic
378 breccias as random. However, we observe a weak tendency for bedded slabs to have low
379 dips, as for instance at St Margaret's Island (loc. 26, Fig. 4e), rather than the typical high dips
380 of host bedrock sequences. This tendency has been tested at eight localities by plotting poles
381 to slab bedding (Fig. 11) and computing the three eigenvectors of the orientation tensor,
382 effectively the axes of maximum, minimum and intermediate concentration of the bedding
383 poles. The distributions have not been rotated in any way, given the evidence that a) the
384 conjugate subvertical cross-faults remain in the orientation in which they were formed, with
385 their mutual intersection vertical and b) geopetal indicators in the breccias are still horizontal.

386 Using the test of Woodcock and Naylor (1983), all the distributions of poles are
387 significantly non-random at the 99% confidence level, except Draught and Bullslaughter
388 west, which are significant at the 95% level. The mean bedding poles mostly lie within 30° of
389 vertical (Fig. 11d), indicating that the bedded slabs themselves lie within 30° of horizontal.
390 Bullslaughter east and Giltar east show slightly higher mean dips, though with confidence
391 areas that allow for 30° mean dips or less. Only at Draught, with a small sample size, do slabs
392 show significantly higher dips.

393 If slabs had been aligned by shear strains parallel to the host fault or bedding plane, then
394 the slabs would tend to align parallel to this controlling shear zone (Fig. 3b), indicated by the
395 great circle on the stereoplots (Figs 11a, b, c). Actually, slabs tend to be oriented more
396 perpendicular than parallel to the controlling zone. The tendency for the slabs to have low
397 dips strongly suggests accumulation under gravity, by collapse of wall rock slabs into an
398 open void formed by karstic solution (Fig. 3a) or, as suggested in this paper, by dilational
399 faulting (Fig. 3c).

400

401 [Figure 11 about here]

402

403

404 **11. Discussion**

405

406 *11.1. Karstic solution and collapse origin for chaotic breccias and megabreccias?*

407

408 This discussion first compares the new observations from the Pembrokeshire breccia zones
409 against the three main formation hypotheses (Walsh et al., 2008). The first comparison is
410 with the original hypothesis of Dixon (1921) that the chaotic breccias and megabreccias
411 represent collapse of the roof and walls of fissures formed by groundwater dissolution of
412 Carboniferous limestone in the Triassic.

413 The present study has certainly found small (0.1 to 1 metre scale) irregular sediment-
414 filled cavities within some breccia zones – for instance at Frank’s Shore (loc. 18) and
415 Valleyfield East (loc. 20) – that can be ascribed to phreatic solution. However, our mapping
416 has confirmed the observations of Thomas (1971) and Walsh et al. (2008) that the margins of
417 the breccia zones lack fluted and scalloped solution surfaces. Instead they are either smooth

418 bedding or fault planes, or grade out through mosaic and crackle breccia into intact limestone.

419 Slickensided clasts are found within some breccias, but derived fluted surfaces are not.

420 Although karstic solution alone is an unlikely origin for the breccia-filled fissures, our
421 measured sub-horizontal clast fabrics (Section 10, Fig. 11) are strong evidence for the second
422 component of Dixon's (1921) hypothesis: gravitational collapse of blocks and slabs into an
423 open void. We merely prefer a dilational tectonic origin for those voids. However, given the
424 increased solubility of fractured limestone in acidic groundwater, such fault zones might
425 naturally suffer localised solution.

426 Bullslaughter Bay (locs 2, 3, 4) has received recent attention (Walsh et al., 2008;
427 Błażejowski and Walsh, 2013; Rowberry et al., 2014) because of a solutional overprint on
428 earlier formed breccias. It is significant that none of the eleven other sites of deep weathering
429 recorded by Rowberry et al. (2014) are associated with chaotic breccias, but rather occur in
430 normally bedded limestones. We therefore regard the solutional overprint at Bullslaughter
431 Bay as affecting breccias formed in the same way as elsewhere in Pembrokeshire: by
432 dilational tectonics followed by collapse.

433

434 *11.2. Phreatic explosion origin for chaotic breccias and megabreccias?*

435

436 The second hypothesis is that of Walsh et al. (2008) that brecciation was due to phreatic
437 explosion. Phreatic activity results from the interaction of magma with external water,
438 creating overpressure that brecciates then erupts the country rock (Tămaş and Milési, 2003).

439 However, their diagnostic criteria for phreatic brecciation do not match well the

440 Pembrokeshire examples:-

- 441 1. Pembroke Group breccia bodies lack the typical shape of phreatic bodies: conical pipes,
442 narrowing downwards, with irregular finger-like contacts. Rather, most bodies are planar

443 (Fig. 7), with only 4 out of 27 being irregular, and none being demonstrably conical. Many
444 have at least some planar contacts.

445 2. Clasts in the studied breccias are mostly angular, whereas phreatic breccias typically have
446 some rounded fragments.

447 3. The studied breccias lack the pervasive siliceous cementation and alteration characteristic
448 of phreatic breccias.

449 4. The matrix in phreatic breccias is the fine-grained fraction from rock brecciation,
450 necessarily deposited at the same time as the larger fragments. By contrast, much of the
451 interclast matrix in the studied breccias is laminated (e.g. Fig. 5c, d) and therefore
452 introduced after the clasts.

453 This evidence, together with the absence of the requisite magmatic heat source in this area,
454 argues against the phreatic brecciation model.

455

456 *11.3. Dilational faulting and collapse origin for chaotic breccias and megabreccias?*

457

458 “Tectonic” hypotheses for Pembroke Group breccia formation were initiated by Thomas
459 (1971) although he was unspecific about the process involved. We suggest that the chaotic
460 breccias and megabreccias resulted from collapse of the walls and roofs of voids formed
461 along dilational faults during regional extension. Minor solutional widening of the void is
462 possible, but no evidence for large-volume solution has been observed. The collapse could
463 have been at the same time as fault displacement, or could have happened between fault
464 episodes. Evidence of polyphase brecciation and cementation is consistent with repeated
465 displacement on some fault zones. Most interclast matrix infiltrated later from above, and
466 residual void space was then filled by carbonate cement.

467 An important factor in the collapse hypothesis is that the final width of the breccia zone is
468 predicted to be over three times the width of the primary fissure (Loucks, 1999). If the wall
469 rocks have zero initial porosity and collapse into a planar void of width W_v , the final width of
470 the breccia body W_b is given by $W_b = W_v/\Phi_b$, where Φ_b is the porosity of the collapse
471 breccia. With a breccia porosity $\Phi_b = 0.3$, a 1 m aperture void would generate a 3.3 m
472 thickness of chaotic breccia. Even a 1 metre wide void exceeds the likely average fault
473 displacement in this area. Using an empirical determined fault displacement/length factor of
474 6.5×10^{-5} (Sibson, 1989; Scholz, 2002) Pembrokeshire faults of the order of 5 km would
475 have a maximum displacement of 0.325 m. Wide zones of collapse breccia would require
476 repeated fault displacements, evidenced by the observed polyphase brecciation and
477 cementation.

478 Evidence for collapse into fault-induced voids is:-

- 479 1. Most of the breccia zones are related to cross-strike faults, marked by dilational crackle
480 and mosaic breccias and by principal slip surfaces, some with low-plunge slickensides.
- 481 2. Clasts of crackle and mosaic breccia are common in the chaotic breccias, representing
482 fragments of faulted wall rock collapsed into the fault void.
- 483 3. Slickensided clasts from the fault walls occur in the chaotic breccias.
- 484 4. The bedded slabs in the megabreccias tend to lie at low dips rather than parallel to
485 margins of the breccia zone, precluding alignment due to zone-parallel fault shear.
- 486 5. Kinked bedding bordering some breccia zones shows one way in which wall rock
487 collapsed into voids.

488 Dilational faulting is less compatible with megabreccia formation during Variscan shortening
489 than during later regional extension. In Section 12.5 Below (section 12.5) we suggest a
490 Triassic or later extension age, coeval with formation of the Bristol Channel Basin.

491 We deduce that dilation occurred on two main types of fault in response to north-south
492 extension. *Dilational strike-slip faults* reactivated the conjugate Variscan faults striking NNE
493 and NNW (Fig. 12a) (Thomas, 1971). For a 60° dihedral angle between faults, every metre of
494 north-south extension across one of these faults would resolve into $\cos 30^\circ = 0.87$ metres of
495 strike-slip and $\sin 30^\circ = 0.5$ metres of dilation. The east-west bedding-parallel breccia zones
496 are seen as the steep segments of *dilational normal faults* opening perpendicular to regional
497 north-south extension (Fig. 12b). We envisage them having listric geometry (Fig. 12c), so
498 dipping less steeply at depth and maybe rooting into reactivated Variscan thrusts. Dilational
499 normal faults are well understood (e.g. Ferrill and Morris, 2003) and have been postulated for
500 sediment-filled fissures in the Pembroke Group of the Mendip Hills, 200 kilometres to the
501 east (Wall and Jenkyns, 2004).

502

503 [Figure 12 about here]

504

505 Most examples of breccia-filled dilational normal faults (localities 15, 16, 26, 29) occur
506 along the steep southern limb of the Pembroke Syncline. Clearly, bed-normal north-south
507 extension will be greatest in these steeply-dipping beds. In moderately-dipping panels of
508 stratigraphy, deep-seated normal faults probably propagated by bedding-plane slip, with less
509 bed-normal dilation.

510

511 *11.4. Objections to a “tectonic” origin for the megabreccia voids?*

512

513 Walsh et al. (2008) have raised a number of objections to the tectonic origin of breccia-
514 filled voids, which we now address.

515 1. A solutional origin for the voids explains why studied megabreccias are restricted to the
516 Pembroke Limestone Group. Walsh et al. (2008) ask *why, if the voids are produced by*
517 *faulting, are they “absent in the equally brittle rocks and complicated Variscan*
518 *structures in the adjacent Old Red Sandstone outcrop?”* The same question can be
519 extended to include the later Carboniferous Marros and Coal Measures groups. An
520 answer is that, although all these units suffered the same Variscan deformation, they are
521 not equally “brittle”. The units above and below the Pembroke Limestone Group are
522 dominated by sandstone and shale. Sandstones tend to be less well cemented than
523 limestones, and therefore to have lower compressive strengths (70 rather than 100 Mpa),
524 tensile strengths (5 rather than 10 MPa) and shear strengths (15 rather than 30 Mpa)
525 (Waltham, 2002). The lower strength of the sandstones means that they tend to creep
526 ductilely, that brittle fractures nucleate at closer spacings, and that any one fracture is less
527 likely to produce a large void. The greater proportion of shale in the Old Red Sandstone
528 and upper Carboniferous units further weakens them. The concentration of breccias
529 within the the strong shale-poor lithologies in the Pembroke Group (Fig. 2) is predicted
530 from other studies of fault rock control by mechanical stratigraphy (e.g. Ferrill and
531 Morris, 2008; Woodcock et al., 2008)

532 2. *“Why are [megabreccia-filled voids] also absent in the Carboniferous Limestone*
533 *outcrops west of the Flimston Fault, in SE Ireland and in the Gower Peninsula?”* In
534 section 12.5, we argue that the void-forming event was the Triassic or later extension that
535 formed the Bristol Channel Basin. Southeast Ireland is more remote from such Mesozoic
536 basins, and the western end of the Pembroke Peninsula seems to have been just outside
537 the zone of basin extension. The Gower Peninsula does have one megabreccia zone at
538 Mewslade (Wright et al., 2009) and many other sediment- and vein-filled dilational
539 faults.

- 540 3. *Why, if the breccia bodies “are largely controlled by the main-phase Variscan fold*
541 *geometry” do the breccias not “follow the cross-faults and fold axes as sheet-like or*
542 *wall-like bodies?”* We have shown that about 23 out of 30 mapped zones are indeed
543 planar sheets. However some geometries are problematic, particularly the relationship of
544 the Whitesheet and Lydstep Point breccia bodies (Fig. 9d) cited by Walsh et al. (2008).
545 These masses involve collapse of two slightly different stratigraphic horizons, which we
546 envisage as overlapping (Fig. 12b) or being separated by cross-strike transfer faults (Fig.
547 9c), like that cutting the Whitesheet mass.
- 548 4. We agree with Walsh et al. that the size and arrangement of the blocks in a megabreccia
549 body such as Trevallen “implies a lodgement from free-fall conditions into a large pre-
550 existing cavity and, as such, is incompatible with Thomas’s origin by “rock-bursting in
551 compressional zones”. We differ from Thomas (1971) in proposing breccia formation
552 during regional extension.

553

554

555 *11.5. Regional pattern of dilational faulting*

556

557 The conclusion that the chaotic breccias were due to fissure collapse during north-south
558 extension begs the question of the age of this event. The geopetal matrix/cement contacts
559 (Fig. 5c) show that fault fissure formation post-dated Variscan (late Carboniferous) folding,
560 and predated a truncating Mid-Miocene planation surface (Walsh et al., 2008). Within this
561 time window, evidence for polyphase breccia formation includes clasts of earlier breccia and
562 their calcite cement, and successive cements of contrasting composition. However regional
563 correlations with analogous extensional fracture systems consistently suggest a late Triassic
564 to early Jurassic age.

565

566

[Figure 13 about here]

567

568 A map of southwest England and south Wales (Fig. 13) plots the location of extensional
569 fracture systems associated with breccias, finer sediments or hydrothermal cements
570 analogous to the Pembroke examples. All but the three southern sites are hosted in Pembroke
571 Group, from Pembrokeshire to the Mendip Hills. The sites border or lie within the Mesozoic
572 Bristol Channel Basin in four main groups.

573 *The Gower Peninsula*, about 30-50 km east of the Pembroke Peninsula, is crossed by the
574 same conjugate strike-slip Variscan cross faults (George, 1940). These faults have also been
575 reactivated in the Pembroke Group with a dilational component, and filled mostly with
576 hematite-calcite veins and laminated red sediment (Wright et al., 2009). One locality
577 (Mewslade, Fig. 14a) has a megabreccia similar to those of the Pembroke Peninsula. The age
578 of the Gower fault fissures is unproven. Wright et al.(2009) suggested a late Variscan age,
579 but we favour the Triassic age suggested by Strahan (1907) on the basis of supposedly
580 Triassic red sandstones unconformably overlying the Pembroke Group at Port Eynon. A later
581 age cannot be ruled out.

582

583

[Figure 14 about here]

584

585 *The Vale of Glamorgan*, about 20-60 km further east again, has a well-dated Triassic to
586 Jurassic cover (Waters and Lawrence, 1987; Wilson et al., 1990) and underlying fissures in
587 the Pembroke Group filled with red sandstone and mudstone (Fig. 13). Some fissures are
588 notable for their vertebrate remains (Benton and Spencer, 1995). Whiteside and Marshall
589 (2008) conclude that most of these fills and analogous examples around Bristol and the

590 Mendips are Rhaetian (latest Triassic). The tectonic setting of the Glamorgan examples is
591 poorly understood, though most seem to be associated with dilational faults (Wilson et al.,
592 1990; Wall and Jenkyns, 2004) with the same Variscan template as further west. No
593 megabreccia has been described. Faults cutting Early Jurassic units are consistent with
594 extension of the Bristol Channel Basin continuing at least till Late Jurassic (Glen et al., 2005)
595 or Early Cretaceous (Holford et al., 2005) time.

596 *The Mendip Hills* lie 15-60 km ESE of Glamorgan, where the Bristol Channel Basin
597 merges with the Wessex Basin (Fig. 13). The eastern Mendips contain sedimentary fissure
598 fills descended from the contemporary land surface or sea bed, or derived from collapse of
599 the fissure walls (Wall and Jenkyns, 2004). There are some chaotic breccias, but no
600 megabreccias. The fills range through late Triassic and early Jurassic. Wall and Jenkyns
601 make a strong case that the fissures are the steep segments of dilational normal faults rather
602 than solution cavities. They deduce a roughly NE-SW maximum extension direction from the
603 spread of late Triassic fissure directions. However, reactivated Variscan strike-slip cross
604 faults have not been distinguished from east-west dip-slip faults, and the kinematic pattern
605 may be simpler than Wall and Jenkyns suggest. Where the Mendip Hills meet the coast (Fig.
606 13, locations Bre, Wor & San), we have observed fault fissures with fills that include calcite-
607 cemented crackle to chaotic breccia, bedded red sandstone, and bedded chaotic breccia (Fig.
608 14b). The fissures comprise both north-south cross faults and east-west dilational normal
609 faults apparently reactivating north-dipping Variscan thrusts. Fissure sediments in boreholes
610 south of the Mendips (Fig. 13, locations Can, Dar & Bru) are undated (e.g. Holloway and
611 Chadwick, 1984).

612 *The Bristol area*, to the north of the Mendips, has sediment-filled fissures containing
613 vertebrate remains (review by Whiteside and Marshall, 2008) at localities such as
614 Tytherington, Cromhall and Durdham Down (Fig. 13). Whiteside and Marshall prefer a

615 solutional origin for these fissures and a late Triassic age for the faunas. The fissures have
616 more irregular margins than the Mendips examples, although some do follow E-W or NW-SE
617 fractures. Boreholes at Beachley and Filton have red marl fissure fill below the Triassic
618 unconformity (Whittard, 1947). A blue clay fissure fill at Lulsgate has a lower Sinemurian
619 (Jurassic) fauna (Donovan, 1958).

620 In addition to the probable late Triassic fissure-fill sites associated with the Bristol
621 Channel Basin, a fifth group, around *Torbay* occurs on the south-western fringe of the
622 Wessex Basin (Fig. 13). These fills are hosted in Middle Devonian Torquay and Brixham
623 Limestone formations. However, the fills include similar red sediment, sparry calcite and
624 cemented or matrix-rich breccias (Fig. 14c) to those in the Pembroke Group. The Shoalstone
625 example was studied in detail by Richter (1966). Matching fissure margins imply an origin as
626 dilational fractures, and cross-cutting relationships between predominant ENE-striking and
627 N-striking sets preclude a solutional origin. Our observations at the other two localities
628 confirm these conclusions, though the main extensional fractures strike more ESE at Hope's
629 Nose. The Triassic age for the sediment fill is based only on a lithological match with the
630 unconformably overlying cover.

631 The conclusion from this regional survey is that dilational fractures at most localities on
632 Figure 13, including Pembrokeshire, formed during Mesozoic extension of the Bristol
633 Channel and Wessex basins. A latest Triassic (Rhaetian) age is favoured for the main
634 extension and sediment fill, though extension probably continued at least till Early
635 Cretaceous. Sand and mud from the Mesozoic land surface infiltrated down the extensional
636 fractures and formed laminated fissure fills or matrix to limestone breccias derived by
637 collapse of the fissure walls. Calcite and hematite were deposited from circulating fluids,
638 probably sourced both hydrothermally and from groundwater.

639

640

641 **12. Conclusions**

642

- 643 1. The studied breccia zones each contain several of the following lithologies: crackle and
644 mosaic breccia, chaotic breccia and megabreccia, laminated sediment and matrix, and
645 carbonate cement.
- 646 2. Of the 30 localities described, 21 have significant bodies of chaotic breccia and 13 of
647 megabreccia.
- 648 3. Of the 27 breccia examples with clear contacts, over half are related to cross-strike faults
649 that originated as Variscan strike-slip faults. Five breccia zones parallel moderately to
650 steeply dipping bedding, three zones parallel east-west thrust-faults, and the remaining
651 four zones have irregular margins.
- 652 4. The margins of some of the fault-hosted chaotic breccias and of all the bedding-parallel
653 breccias are sharp and match across the breccia zone, arguing for dilational faulting rather
654 than a solutional origin.
- 655 5. Slickensides within cross-strike breccia zones and polyphase brecciation and cementation
656 also favour the fault-related origin.
- 657 6. Megabreccia slabs tend to have low dips rather than to parallel the host-rock bedding or
658 the breccia-zone margins. This geometry suggests collapse of the walls of open voids
659 along the dilational faults.
- 660 7. Episodes of karstic weathering that overprint breccias at Bullslaughter Bay are not
661 observed in other breccia zones, and are not the primary reason for their formation.
- 662 8. The structural template for the breccia zones was the Variscan (late Carboniferous) east-
663 west folds and thrust faults and the strike-slip cross faults, all due to north-south
664 shortening. The dilational faulting resulted from later north-south extension, reactivating

665 the cross-faults in transtension, and using the folded bedding for the steep dilational
666 segments of listric normal faults.

667 9. The Pembroke Peninsula fissures have geometric analogues along-strike to the east, in
668 Gower, Glamorgan, the Mendips and around Bristol. The eastern examples are due to late
669 Triassic north-south extension of the Bristol Channel Basin, and this is proposed as the
670 most likely age for the Pembrokeshire fissures.

671

672

673 **Acknowledgements**

674

675 This paper derives from undergraduate projects by Alex Miller and Chris Woodhouse,
676 coordinated by Nigel Woodcock. We thank Tony Abrahams, Nick Butterfield, Jason Day,
677 Tony Dickson, Liz Harper, Chris Jeans and Martin Walker for laboratory assistance, Peter
678 Walsh, Matt Rowberry, Richard Walker and Błażej Błażejowski for helpful discussions, Sid
679 Howells for supplying coastal photography and for enabling observation of breccia bodies
680 from kayaks, and Richard Walker and David Ferrill for helpful reviews.

681

682

683

684 **References**

685

686 Anderson, E.M., 1951. The dynamics of faulting, 2nd ed. Oliver & Boyd, Edinburgh,
687 London.

688 Benton, M., Spencer, P.S., 1995. Fossil reptiles of Great Britain, Geological Conservation
689 Review Series,. Joint Nature Conservation Committee, Peterborough, p. 386.

690 Błażejowski, B., Walsh, P., 2013. A Visean (Brigantian) conodont assemblage preserved in
691 the dissolution residue component of a breccia matrix at Bullslaughter Bay, South
692 Wales. Neues Jahrbuch für Geologie und Paläontologie 267, 239-254.

693 Bons, P.D., 2001. The formation of large quartz veins by rapid ascent of fluids in mobile
694 hydrofractures. Tectonophysics 336, 1-17.

695 British Geological Survey, 1977. Pembroke and Linney Head, England & Wales Sheet 244
696 & 245, 1:50,000 Series. British Geological Survey, Keyworth, Nottingham.

697 British Geological Survey, 1996. Tectonic map of Britain, Ireland and adjacent areas. British
698 Geological Survey, Keyworth, Nottingham.

699 Dixon, E.E.L., 1921. The geology of the South Wales Coalfield, Part XIII: The country
700 around Pembroke and Tenby, Memoir, Geological Survey of the United Kingdom.
701 H.M.S.O.

702 Donovan, D.T., 1958. Easter Field Meeting: The lower and middle Jurassic rocks of the
703 Bristol district. Proceedings of the Geologists' Association 69, 130-140.

704 Dubois, C., Quinif, Y., Baele, J.-M., Barriquand, L., Bini, A., Bruxelles, L., Dandurand, G.,
705 Havron, C., Kaufmann, O., Lans, B., Maire, R., Martin, J., Rodet, J., Rowberry, M.D.,
706 Tognini, P., Vergari, A., 2014. The process of ghost rock karstification and its role in
707 the formation of cave systems. Earth Science Reviews 131, 116-148.

708 Ferrill, D.A., Morris, A.P., 2003. Dilational normal faults. *Journal of Structural Geology* 25,
709 183-196.

710 Ferrill, D.A., Morris, A.P., 2008. Fault zone deformation controlled by carbonate mechanical
711 stratigraphy, Balcones fault system, Texas. *American Association of Petroleum*
712 *Geologists Bulletin* 92, 359-380.

713 Ferrill, D.A., Wyrick, D.Y., Smart, K.J., 2011. Coseismic, dilational-fault and extension-
714 fracture related pit chain formation in Iceland: analog for pit chains on Mars.
715 *Lithosphere* 3, 133-142.

716 Frenzel, M., Woodcock, N.H., in press. Cockade breccia: product of mineralisation along
717 dilational faults. *Journal of Structural Geology*.

718 Genna, A., Jébrak, M., Marcoux, E., Milési, J.P., 1996. Genesis of cockade breccias in the
719 tectonic evolution of the Cirotan epithermal gold system, West Java. *Canadian*
720 *Journal of Earth Sciences* 33, 93-102.

721 George, T.N., 1940. The structure of Gower. *Quarterly Journal of the Geological Society*,
722 London 96, 131-198.

723 Glen, R.A., Hancock, P.L., Whittaker, A., 2005. Basin inversion by distributed deformation:
724 the southern margin of the Bristol Channel Basin, England. *Journal of Structural*
725 *Geology* 27, 2113–2134.

726 Hancock, P.L., 1964. The relations between folds and late-formed joints in South
727 Pembrokeshire. *Geological Magazine* 101, 174-184.

728 Higgins, M.W., 1971. Cataclastic rocks, Professional Paper, United States Geological Survey,
729 p. 97.

730 Holford, S.P., Turner, J.P., Green, P.F., 2005. Reconstructing the Mesozoic–Cenozoic
731 exhumation history of the Irish Sea basin system using apatite fission track analysis
732 and vitrinite reflectance data, in: Doré, A.G., Vining, B.A. (Eds.), *Petroleum Geology:*

733 North-West Europe and Global Perspectives — Proceedings of the 6th Petroleum
734 Geology Conference. Geological Society, London, pp. 1095–1107.

735 Holloway, S., Chadwick, R.A., 1984. The IGS Bruton borehole (Somerset, England) and its
736 regional structural significance. *Proceedings of the Geologists' Association* 95, 165-
737 174.

738 Laznicka, P., 1988. Breccias and coarse fragmentites. *Petrology, environments, associations,*
739 *ores. Developments in Economic Geology*, 25.

740 Loucks, R.G., 1999. Paleocave carbonate reservoirs: origins, burial-depth modifications,
741 spatial complexity, and reservoir implications. *American Association of Petroleum*
742 *Geologists Bulletin* 83, 1795-1834.

743 Mort, K., Woodcock, N.H., 2008. Quantifying fault breccia geometry: Dent Fault, NW
744 England. *Journal of Structural Geology* 30, 701-709.

745 North American Geologic-map Data Model Science Language Technical Team, 2004. Report
746 on progress to develop a North American science-language standard for digital
747 geologic-map databases, in: Soller, D.R. (Ed.), *U. S. Geological Survey Open File*
748 *Report*, <http://www.nadm-geo.org/slitt/products.html> ed, pp. 85-94.

749 Oliver, N.H.S., Bons, P.D., 2001. Mechanisms of fluid flow and fluid-rock interaction in
750 fossil metamorphic hydrothermal systems inferred from vein-wallrock patterns,
751 geometry and microstructure. *Geofluids* 1, 137-162.

752 Phillips, W.J., 1972. Hydraulic fracturing and mineralization. *Journal of the Geological*
753 *Society, London* 128, 337-359.

754 Richter, D., 1966. On the New Red Sandstone dykes of the Tor Bay area (Devonshire).
755 *Proceedings of the Geologists' Association* 77, 173-186.

756 Rowberry, M.D., Battiau-Queney, Y., Walsh, P., Błażejowski, B., Bout-Roumazeilles, V.,
757 Trentesaux, A., Křížová, L., Griffiths, H., 2014. The weathered Carboniferous

758 Limestone at Bullslaughter Bay, South Wales: the first example of ghost rock
759 recorded in the British Isles. *Geologica Belgica* 17, 33-42.

760 Scholz, C.H., 2002. *The mechanics of earthquakes and faulting*, 2nd Edition ed. Cambridge
761 University Press, Cambridge.

762 Sibson, R.H., 1986. Brecciation processes in fault zones: inferences from earthquake
763 rupturing. *Pure and Applied Geophysics* 124, 159-175.

764 Sibson, R.H., 1989. Earthquake faulting as a structural process. *Journal of Structural Geology*
765 11, 1-14.

766 Strahan, A., 1907. *The geology of the South Wales Coalfield, Part IX, West Gower, and the*
767 *country around Pembrey, Memoir, Geological Survey of Great Britain. H.M.S.O.,*
768 *London.*

769 Tămaş, C.G., Milési, J.-P., 2003. Hydrothermal breccia pipe structures – general features and
770 genetic criteria – II. Phreatic breccias. *Studia Universitatis Babeş-Bolyai, Geologia*
771 48, 55-66.

772 Thomas, T.M., 1970. Field meeting of the South Wales group on the Stack Rocks to
773 Bullslaughter Bay section of the South Pembrokeshire coast. *Proceedings of the*
774 *Geologists' Association* 81, 241-248.

775 Thomas, T.M., 1971. Gash-breccias of South Pembrokeshire: fossil karstic phenomena?
776 *Transactions of the Institute of British Geographers* 54, 89-100.

777 Walker, R.J., Holdsworth, R.E., Imber, J., Ellis, D., 2011. The development of cavities and
778 clastic infills along fault-related fractures in Tertiary basalts on the NE Atlantic
779 margin. *Journal of Structural Geology* 33, 92-106.

780 Wall, G.R.T., Jenkyns, H.C., 2004. The age, origin and tectonic significance of Mesozoic
781 sediment-filled fissures in the Mendip Hills (SW England): implications for extension
782 models and Jurassic sea-level curves. *Geological Magazine* 141, 471-504.

783 Walsh, P., Battiau-Queney, Y., Howells, S., Ollier, C., Rowberry, M., 2008. The gash
784 breccias of the Pembroke Peninsula, SW Wales. *Geology Today* 24, 137-145.

785 Waltham, A.C., 2002. *Foundations of engineering geology*. 2nd edition. Taylor & Francis,
786 London.

787 Waters, R.A., Lawrence, D.J.D., 1987. *Geology of the South Wales Coalfield, Part III, the*
788 *country around Cardiff*. Memoir, British Geological Survey, Her Majesty's Stationery
789 Office, London.

790 Whiteside, D.I., Marshall, J.E.A., 2008. The age, fauna and palaeoenvironment of the Late
791 Triassic fissure deposits of Tytherington, South Gloucestershire, UK. *Geological*
792 *Magazine* 145, 105-147.

793 Whittard, W.F., 1947. Records of boreholes sunk for the new Severn and Wye bridges.
794 *Proceedings of the Bristol Naturalists' Society* 27, 311-328.

795 Wilson, D., Davies, J.R., Fletcher, C.J.N., Smith, M., 1990. *Geology of the South Wales*
796 *Coalfield, Part VI, the country around Bridgend*. Memoir, British Geological Survey,
797 Her Majesty's Stationery Office, London.

798 Woodcock, N.H., 1977. Specification of fabric shapes using an eigenvalue method.
799 *Geological Society of America Bulletin* 88, 1231-1236.

800 Woodcock, N.H., Mort, K., 2008. Classification of fault breccias and related fault rocks.
801 *Geological Magazine* 145, 435-440.

802 Woodcock, N.H., Naylor, M.A., 1983. Randomness testing in three-dimensional orientation
803 data. *Journal of Structural Geology* 5, 539-548.

804 Woodcock, N.H., Omma, J.E., Dickson, J.A.D., 2006. Chaotic breccia along the Dent Fault,
805 NW England: implosion or collapse of a fault void? *Journal of the Geological Society*,
806 London 163, 431-446.

807 Woodcock, N.H., Sayers, N.J., Dickson, J.A.D., 2008. Fluid flow history from damage zone
808 cements near the Dent and Rawthey faults, NW England. *Journal of the Geological*
809 *Society*, London 165, 829-837.

810 Wright, V., Woodcock, N.H., Dickson, J.A.D., 2009. Fissure fills along faults: Variscan
811 examples from Gower, South Wales. *Geological Magazine* 146, 890-902.

812

813

814

815 **Figure captions**

816

817 **Fig. 1.** a) Geological map of the Pembroke Peninsula, southwest Wales, with breccia
818 localities discussed in the text. Map based on British Geological Survey (1977) but with the
819 Flimston Bay Fault modified to join to the NNW with the easternmost Castlemartin Fault
820 rather than the Freshwater West Fault. b) Location and geological context of main map

821

822 **Fig. 2.** Stratigraphic distribution of breccia in a) the St Florence and Pembroke Synclines and
823 b) the Bullslaughter Bay Syncline. Key and scale (inset bottom right) applies to both areas.

824

825 **Fig. 3.** Schematic diagram of four types of breccia formation mechanism.

826

827 **Fig. 4.** Examples of breccia zone lithologies. a) crackle breccia, Proud Giltar (loc. 17); b)
828 mosaic breccia, Giltar West (loc. 21); c) chaotic breccia, Bullslaughter east (loc. 3); d)
829 chaotic megabreccia, Trevalen (loc. 7); e) chaotic megabreccia, St Margaret's Island (loc.
830 26); f) cataclasite, Stackpole Quay (loc. 12).

831

832 **Fig. 5.** Examples of cement and matrix infill to breccia bodies. a) blocky calcite(left) and
833 elongate calcite (right), Valleyfield East (loc. 20); b) calcite spar ball, Whitesheet (loc. 15); c)
834 laminated (catenary) sand/silt infill to breccia, Bullslaughter south (loc. 4); d) geopetal
835 sediment and cement infill to breccia, Trevalen (loc. 7); e) catenary-bedded micrite, Draught
836 Cove (loc. 14); f) either 'ghost karst' or bedded sediment with dropstones (see text),
837 Bullslaughter south (loc. 4).

838

839 **Fig. 6.** Breccia zone characteristics and infill lithologies at each of the studied localities
840 (numbered on Fig. 1), arranged by structural setting (see text).

841

842 **Fig. 7.** Triangular diagram of contact relations of the studied breccia bodies, as numbered on
843 Fig. 1. End member geometries are illustrated by thumbnail geological maps.

844

845 **Fig. 8.** Maps and photographs of representative breccia zones related to vertical cross faults.
846 a) and b) Raming Hole (loc. 10); c) and d) Stackpole Quay (loc 12); e) and f) Flimston (loc.
847 1). All photos taken looking north. Photos (b) and (f) were taken by Sid Howells.

848

849 **Fig. 9.** Maps and photos of strike-parallel breccia zones: a) Tenby east (loc. 25) (with the
850 Tenby west, loc. 24, simple strike-slip zone); b) and c) Nanna's Cave (loc. 29); d-g)
851 Whitesheet (loc. 15) and Lydstep Point (loc 16). Photos (c), (d) and (g) were taken looking
852 west and photo (f) looking east. Photo (g) was taken by Sid Howells.

853

854 **Fig. 10.** a) Map of the breccia zones at Bullslaughter Bay west, east and south (locs 2, 3 &
855 4). b) and c) Photo-montages of Bullslaughter Bay west (b) and east (c). Photos were taken
856 by Sid Howells.

857

858 **Fig. 11.** Lower hemisphere equal-area plots of poles to bedded slabs in a) cross-strike fault
859 zones b) irregular zones, and c) bedding sub-parallel zones. Mean bedding poles and their
860 95% confidence areas are shown for each distribution, and d) aggregated on one comparison
861 plot. e) The shape and strength of each distribution shown on a plot of the ratios of their
862 eigenvalues (Woodcock, 1977).

863

864 **Fig. 12.** a) Diagrammatic map of folds and conjugate strike-slip faults formed by north-south
865 Variscan shortening. b) Map of postulated post-Variscan north-south extensional reactivation
866 of Variscan faults and steepened bedding. c) Cross-section across a dilational normal fault
867 that steepens to parallel bedding at shallow depths.

868

869 **Fig. 13.** Map of the depositional limits and faults of the Mesozoic Bristol Channel Basin and
870 the western end of the Wessex Basin, with localities of probable late Triassic fissure fills.
871 Faults are from British Geological Survey (1996), and fissure localities mainly from Wall and
872 Jenkyns (2004), Whiteside and Marshall (2008) and Wright et al. (2009).

873

874 **Fig. 14.** Field photographs of probable late Triassic fissure fills from other areas around the
875 Bristol Channel and Wessex Basins (Fig. 13). a) Chaotic megabreccia, Mewslade, Gower
876 Peninsula; b) Bedded chaotic breccia in dilational fault, Worlebury shore, Somerset; d)
877 Sediment fills and calcite-hematite veins in Devonian limestone, Berry Head Quarry, Devon.

878

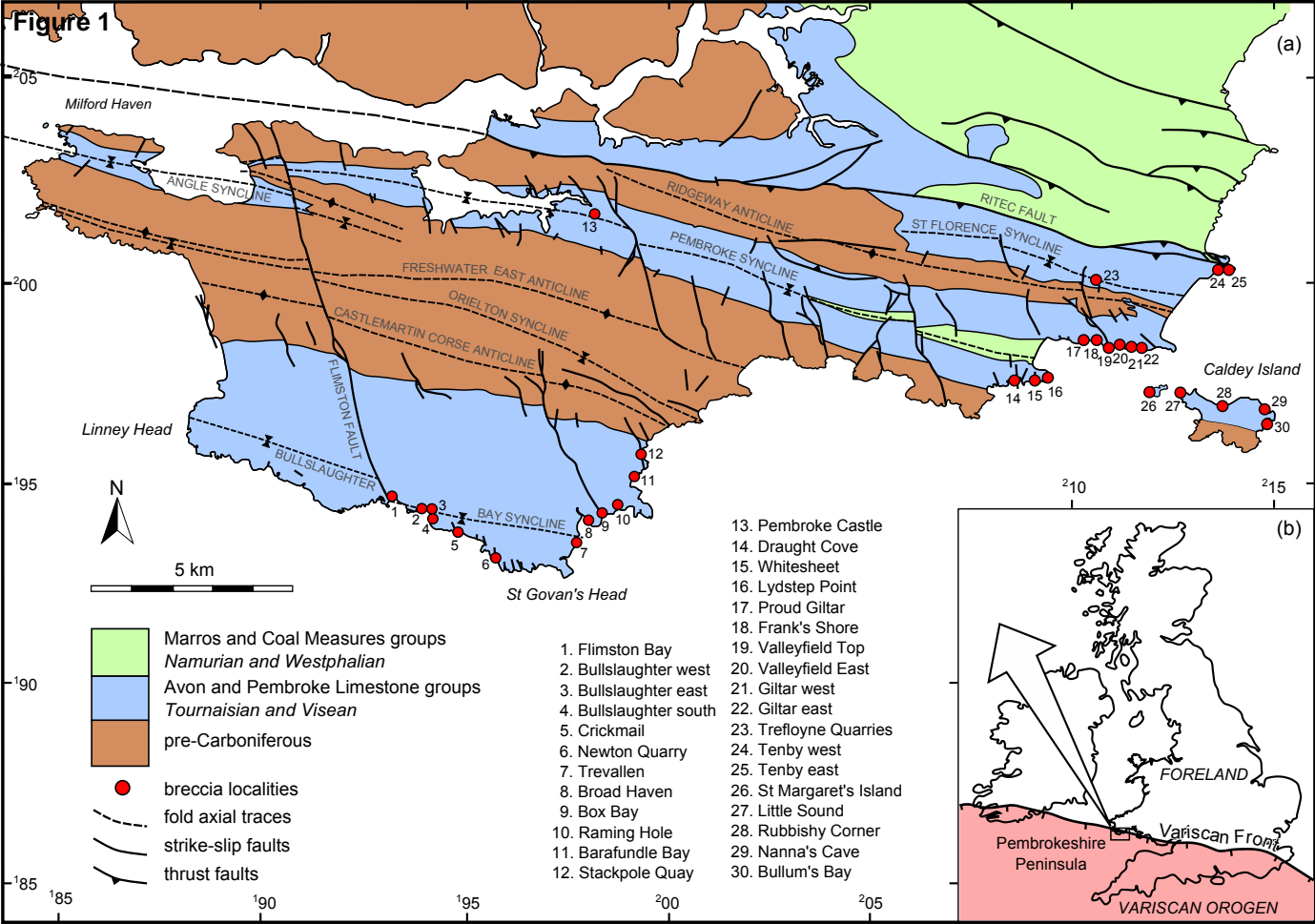


Figure 2

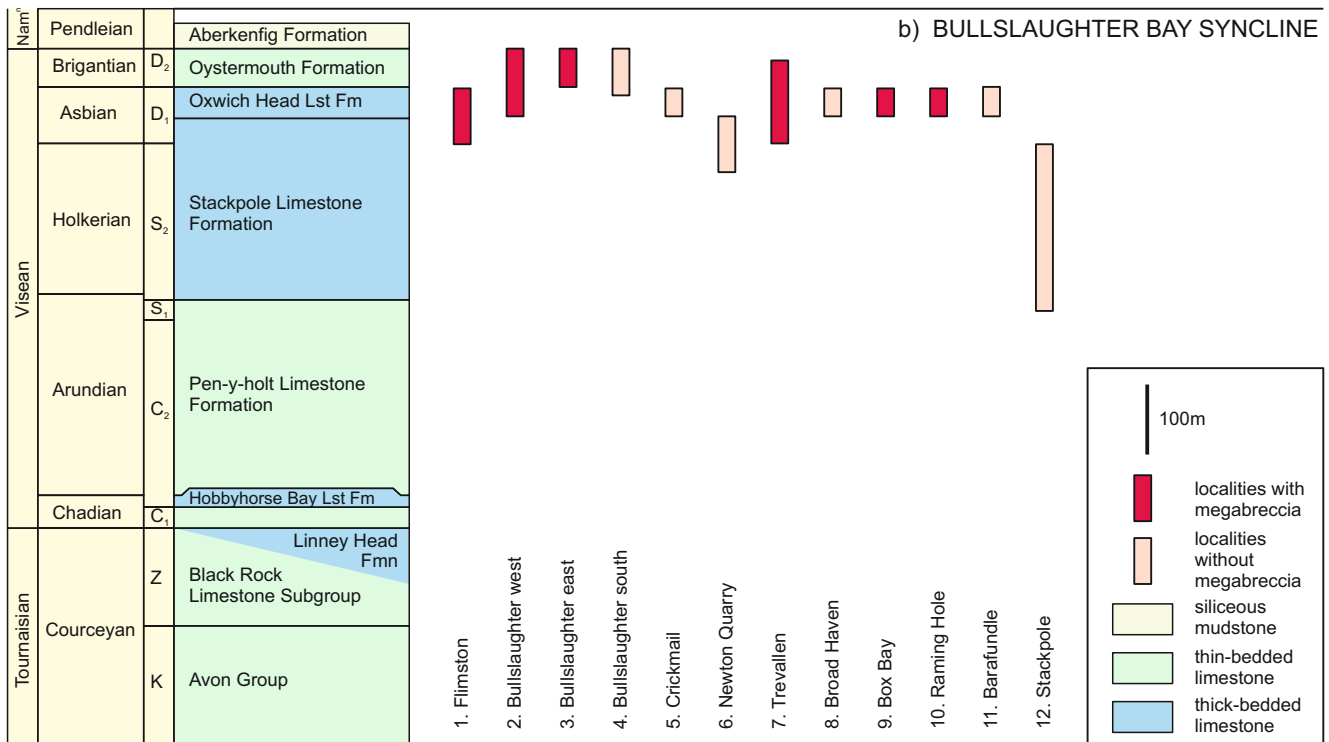
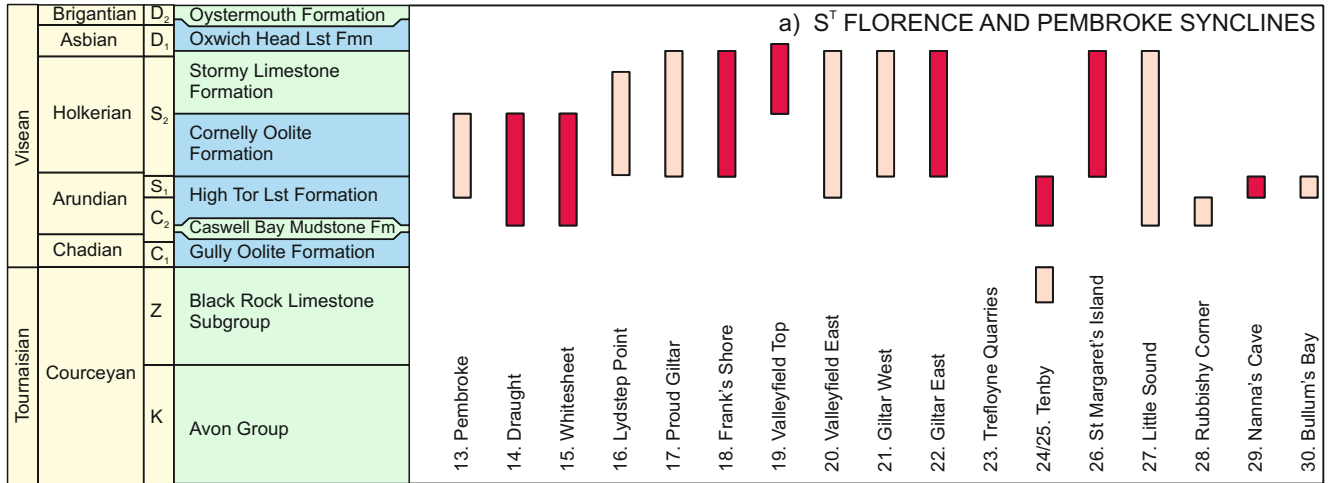
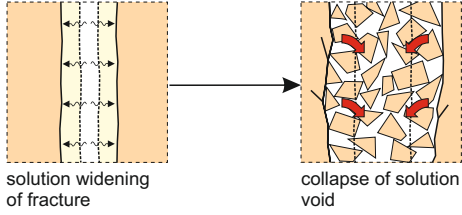
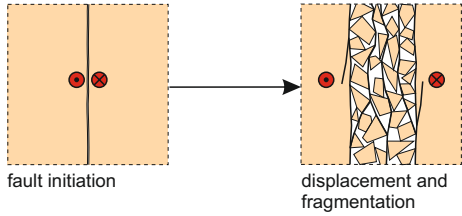


Figure 3

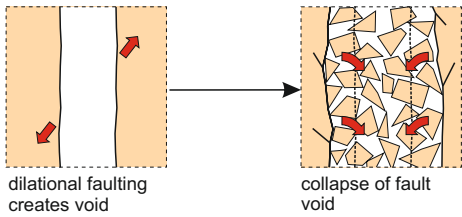
a) karstic solution then collapse



b) fault displacement and fragmentation



c) dilational faulting then collapse



d) phreatic explosion

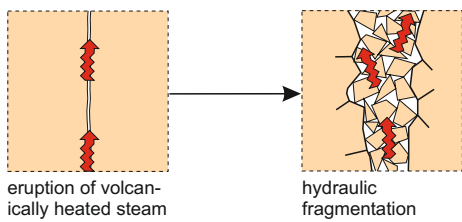


Figure 4



Figure 5



Figure 6

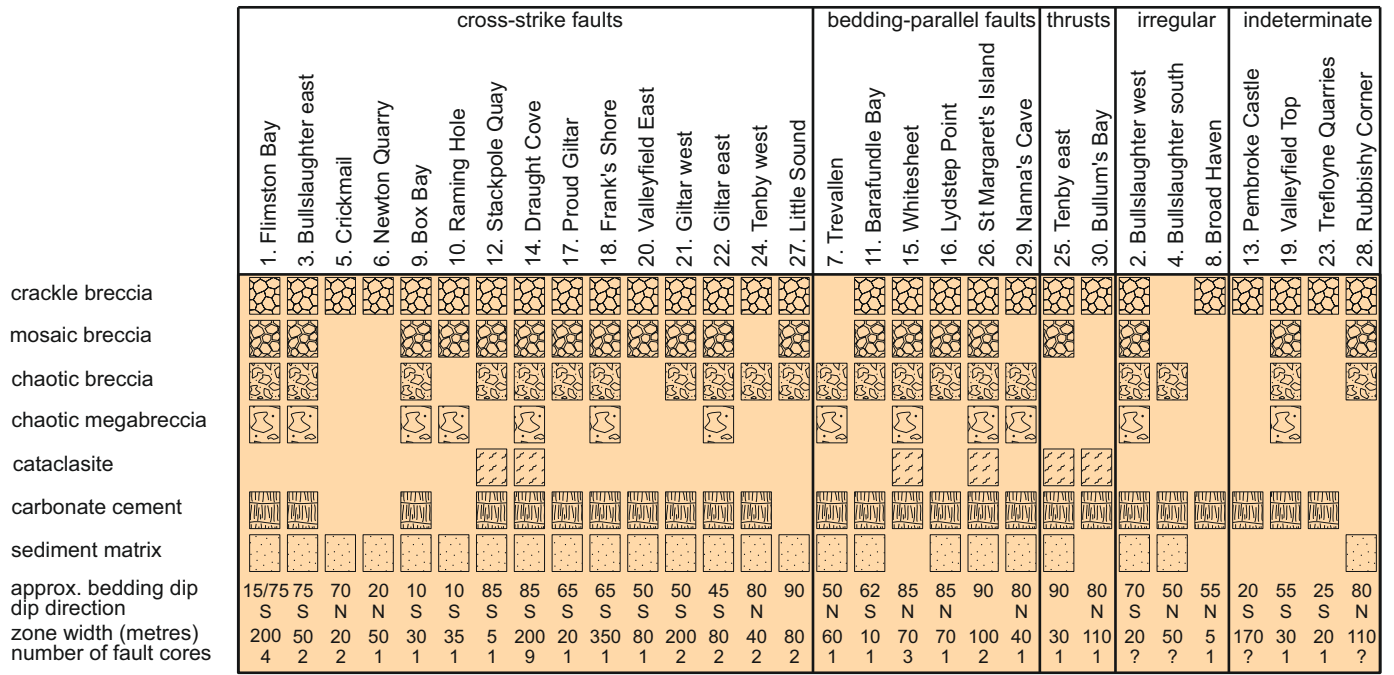
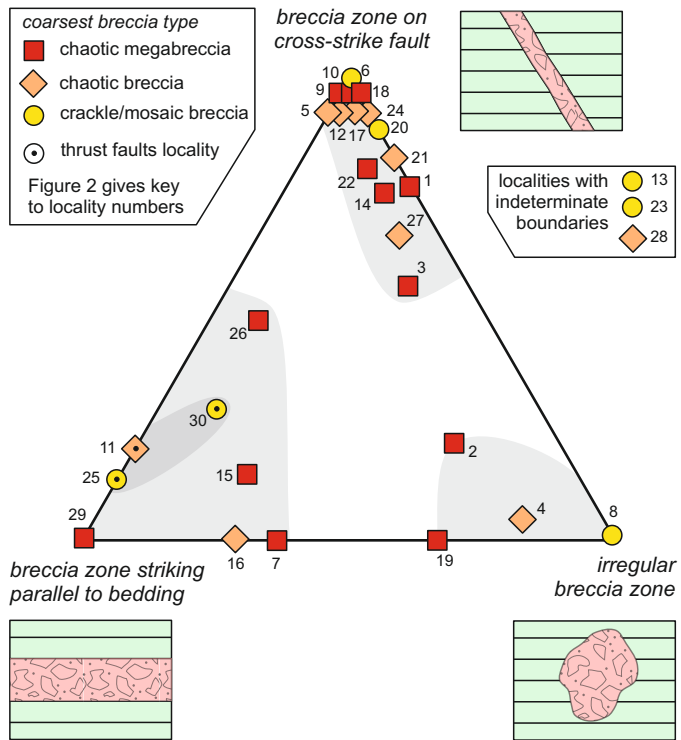
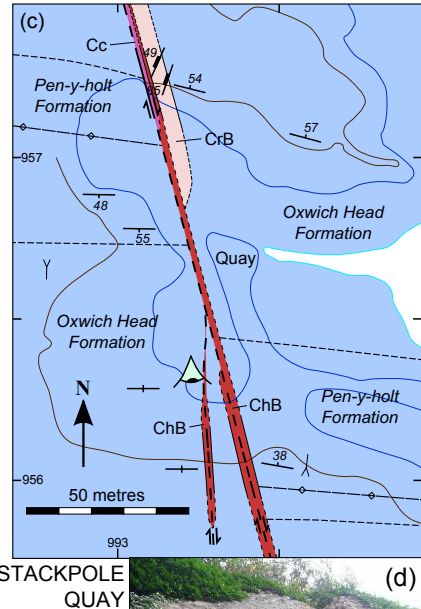
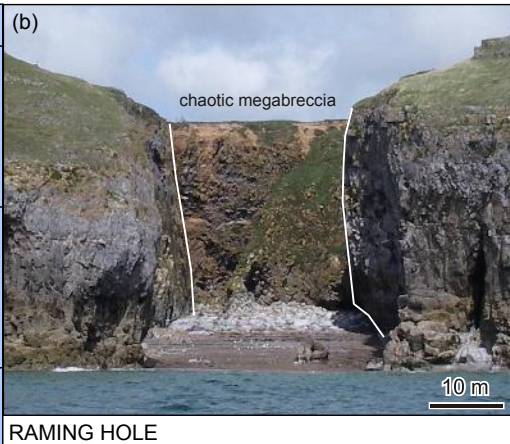
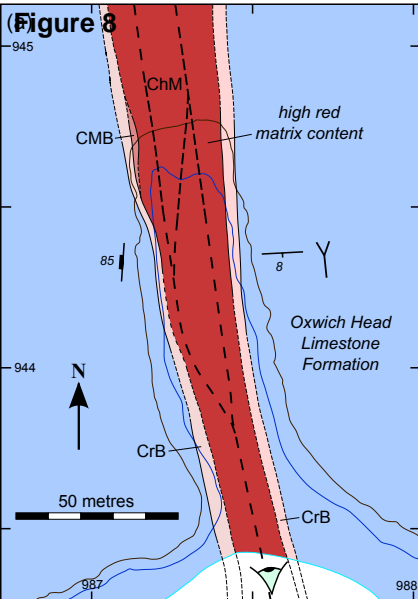
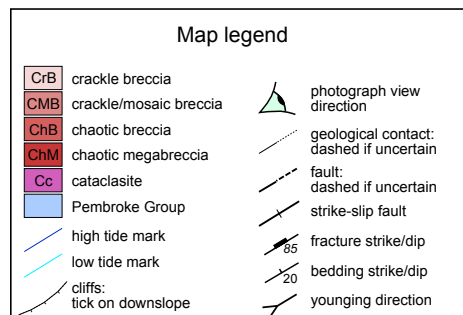
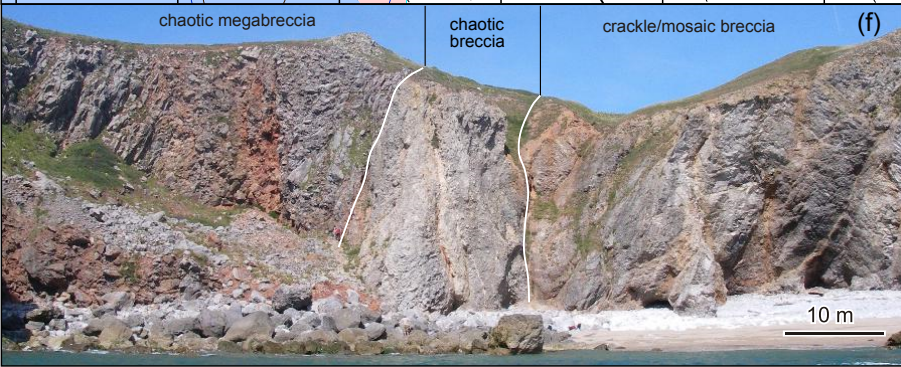
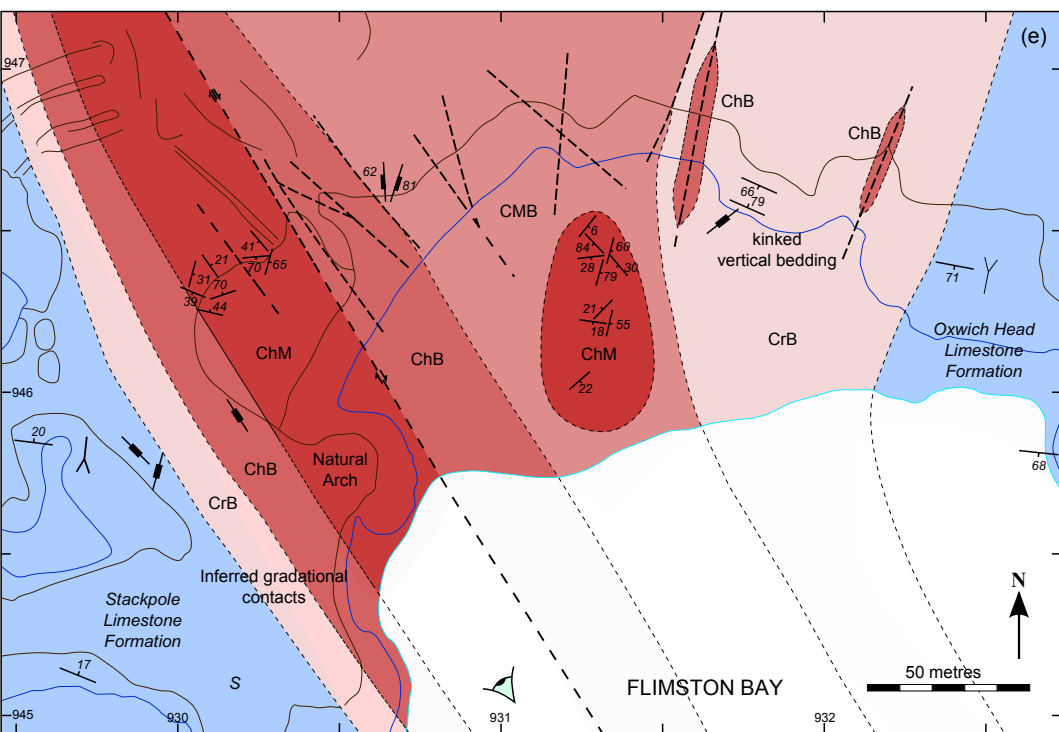
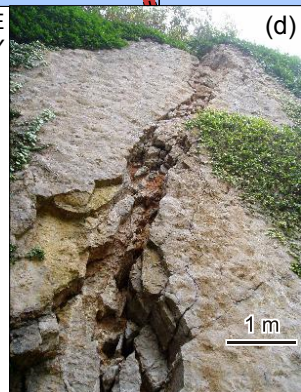


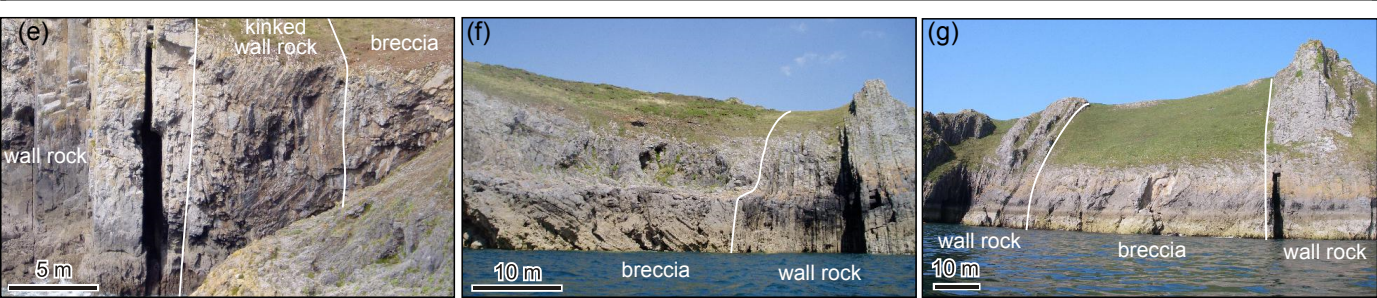
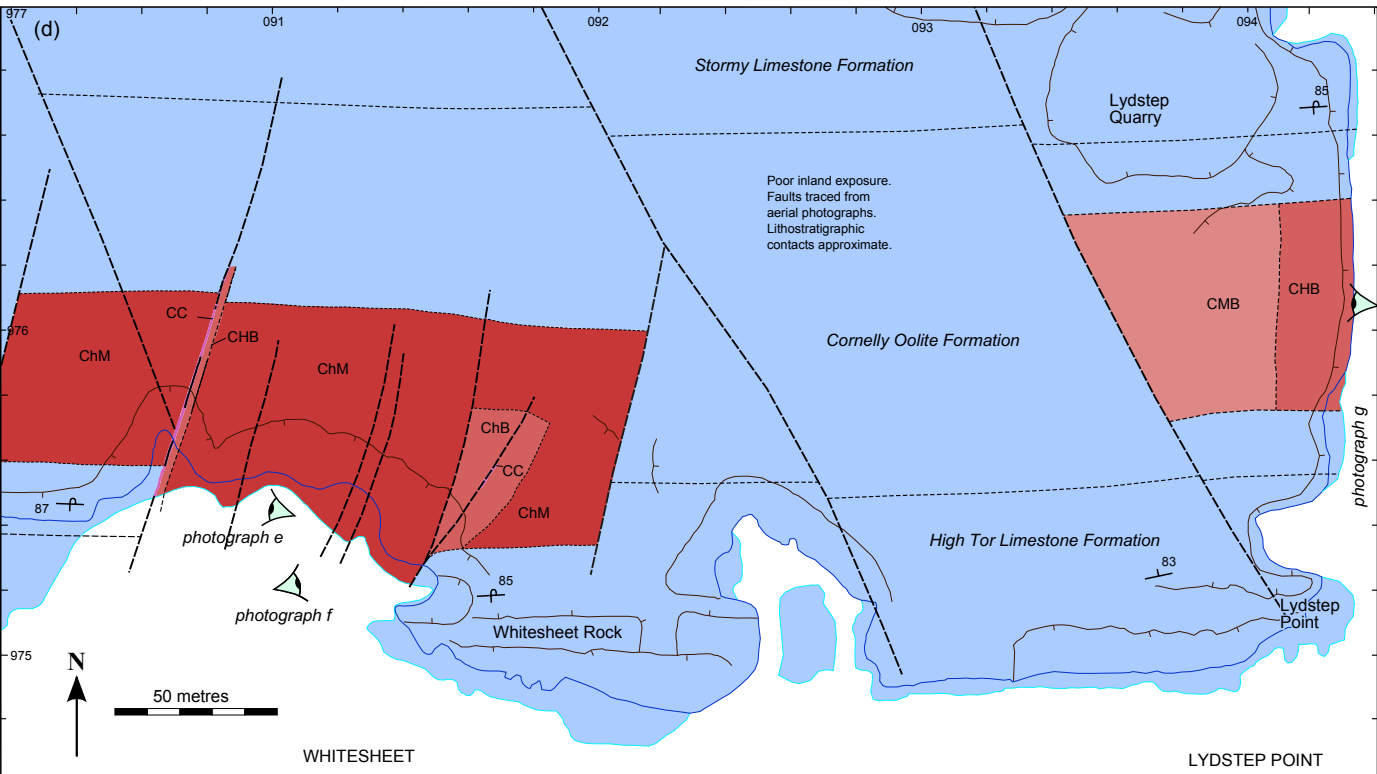
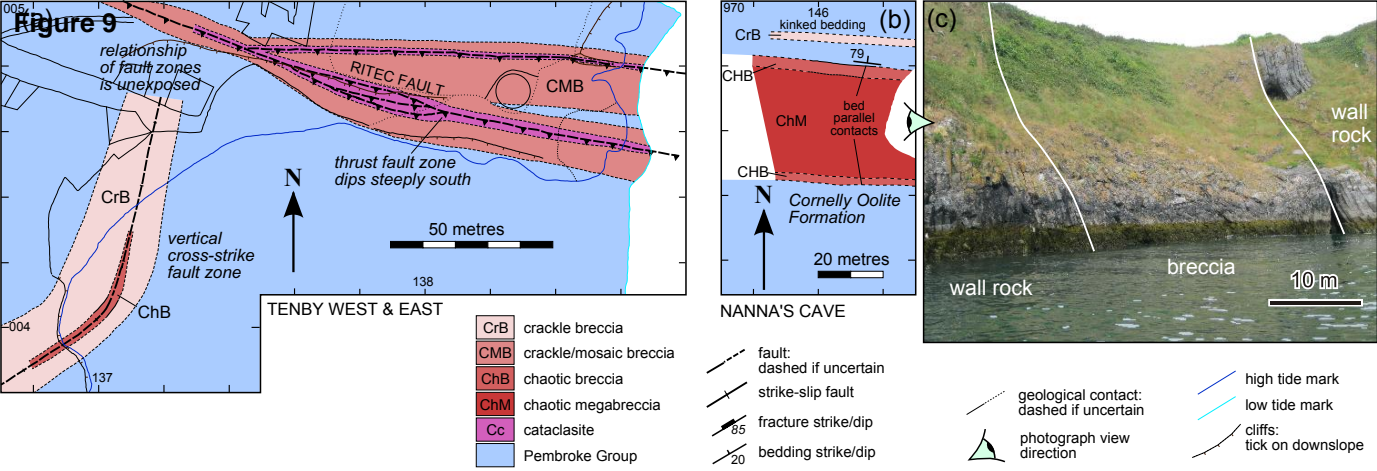
Figure 7





STACKPOLE QUAY





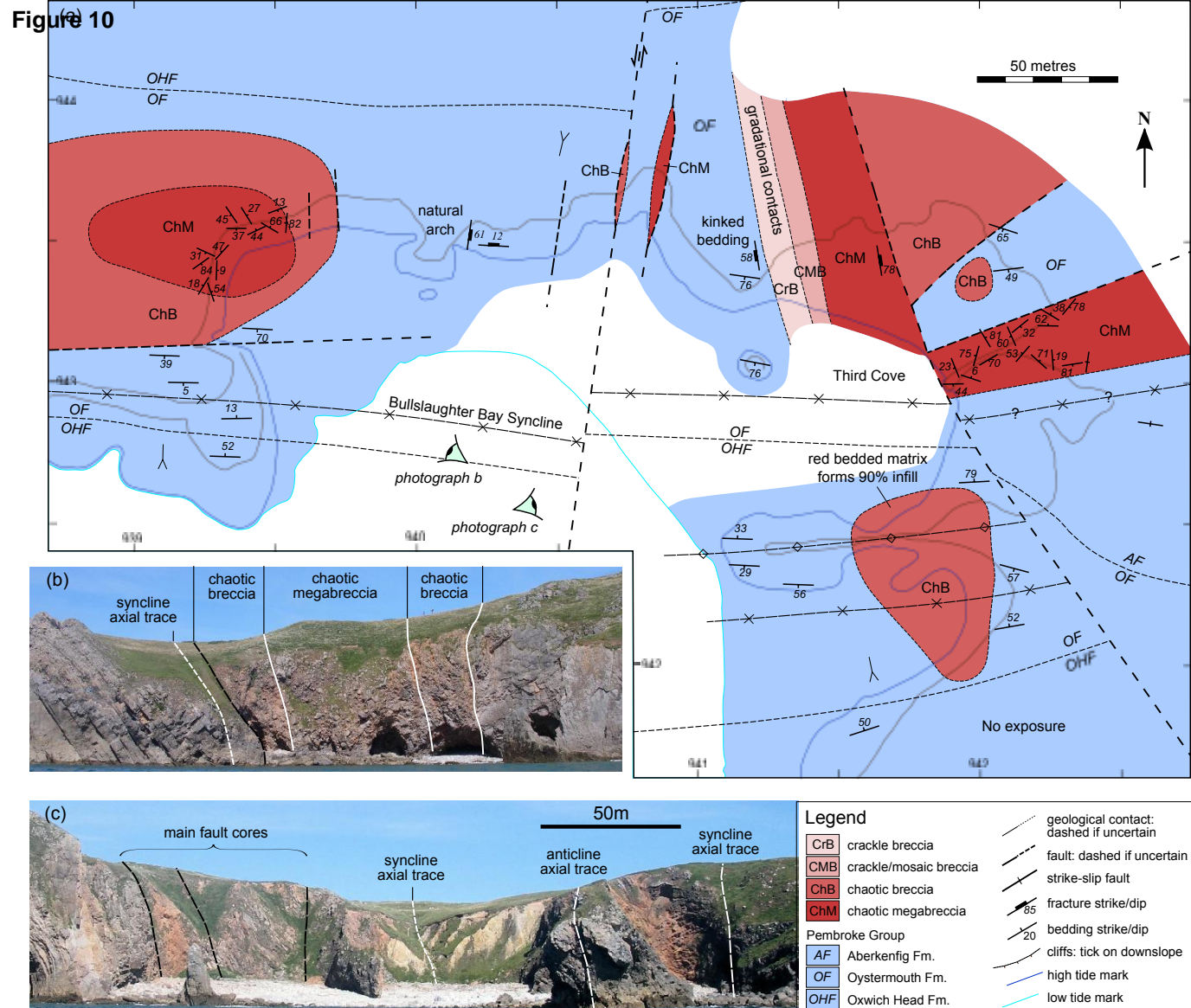
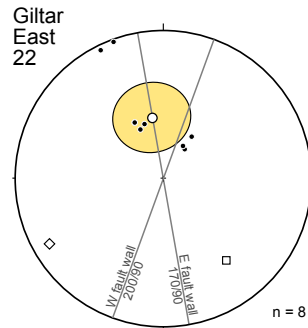
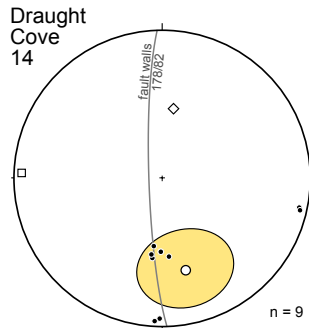
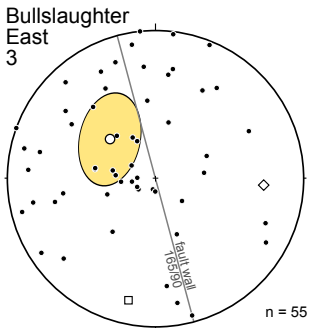
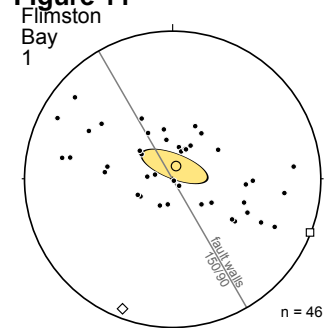
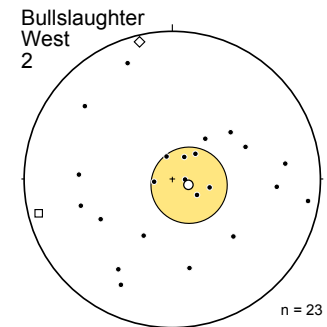


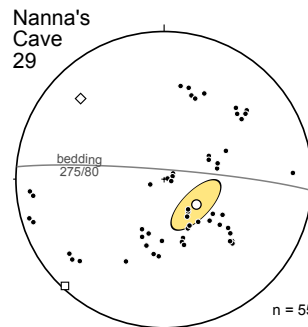
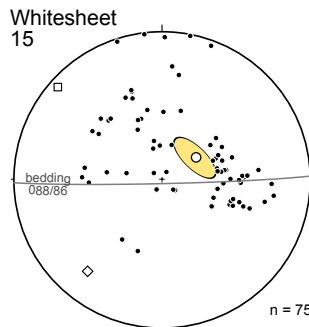
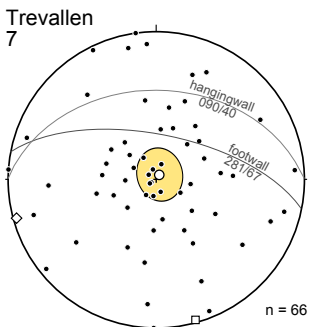
Figure 11



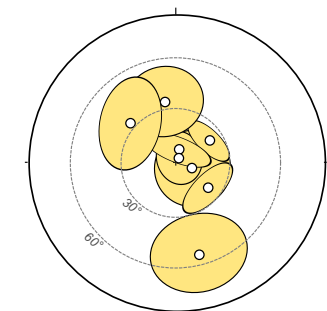
b) Irregular megabreccias



c) Bedding sub-parallel megabreccias



d) Mean bedding poles



Key to stereoplots

- pole to bedded slab
- 1 } eigenvectors
- 2 }
- ◇ 3 }
- 95% confidence ellipse around mean
- great circle trace of bounding bedding or faults
- - - equal dip lines on stereonet

e) Shape/strength plot

1. Flimston
2. Bullslaughter W
3. Bullslaughter E
7. Trevallen
14. Draught
15. Whitesheet
22. Giltar East
29. Nanna's Cave

Shape parameter

$$k = \frac{\ln(S_1/S_2)}{\ln(S_2/S_3)}$$

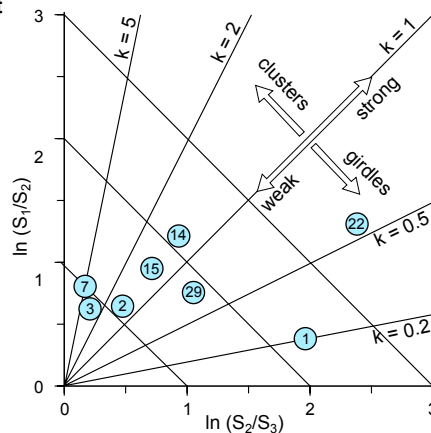
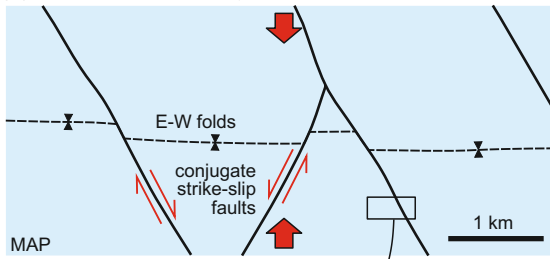
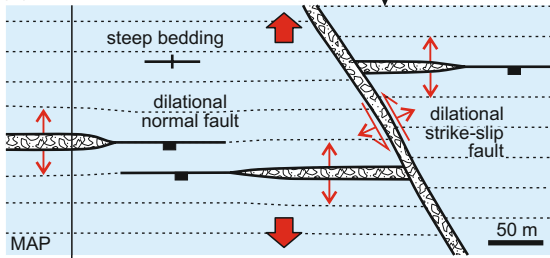


Figure 12

(a) Variscan shortening



(b) late or post-Variscan extension



(c)

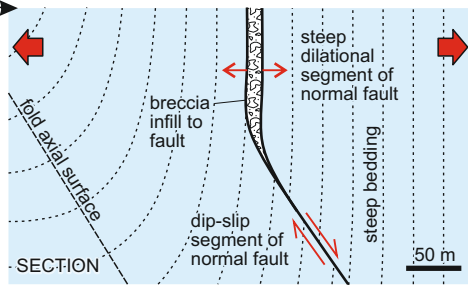


Figure 13

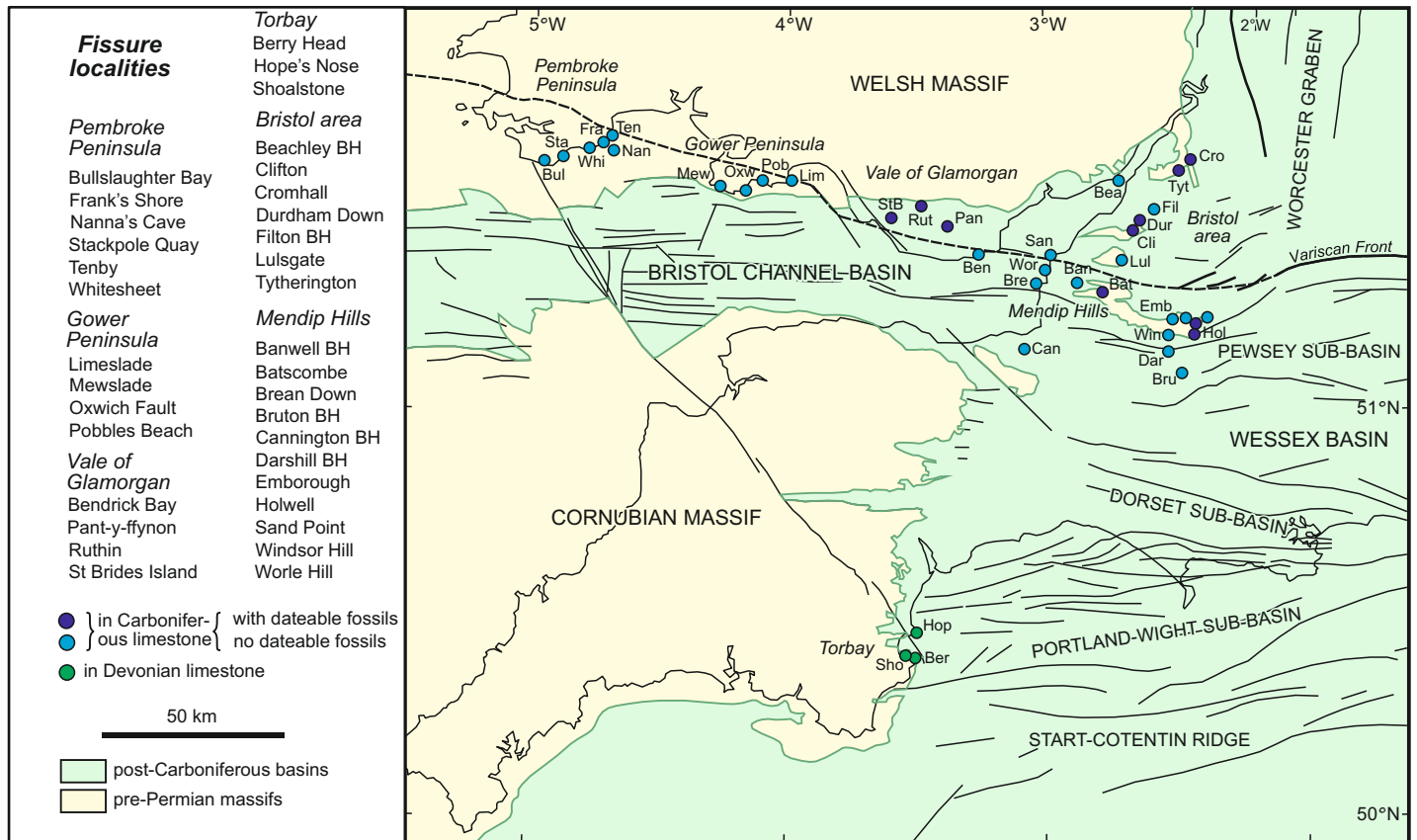


Figure 14

